Supporting Information

Van Eps et al. 10.1073/pnas.1105810108

SI Methods.

Membrane Binding Assays.

$G_{\alpha i}$ (5 μM) subunits were preincubated with $G_{\beta\gamma}$ (10 μM) subunits on ice for 10 min. Then, in the dark, rhodopsin (50 μM) within native membranes was added to the heterotrimetric G protein in a buffer containing 50 mM Tris (pH 8.0), 100 mM NaCl, 1 mM $MgCl_2$ and incubated on ice for 5 min. For dark measurements, reaction mixtures were protected from light for the rest of the procedure. Light activated samples, as well as light activated samples with GTPγS (100 μM), were incubated on ice for 30 min. The membranes in each treatment (dark, light, and light plus GTPγS) were pelleted by centrifugation at 20,000 × *g* for 1 h at 4 °C, and supernatants were removed from pellets. For the dark samples, supernatants were removed under dim red light. The supernatants and pellets of each treatment were boiled and resolved by SDS-PAGE. The protein samples were visualized with Coomassie blue and quantified by densitometry using a BioRad Multimager. Each sample was evaluated by comparison of the amount of $G_{\alpha i}$ subunits in pellet (P) or supernatant (S) to the total amount of $G_{\alpha i}$ subunits (P+S) in both treatments and expressed as a percentage of the total $G_{\alpha i}$ protein. Results are averages from at least three independent experiments. Results are shown in Fig. S2*A*.

Modeling of the Complex Based on Available Information, Including DEER Distances.

Comparative Model of the Heterotrimeric G-Protein Transducin with $G_{\alpha i}$ Sequence. The structure of the heterotrimeric G-protein transducin (PDB ID code 1GOT) was used as a template. The heterotrimeric protein consists of three subunits, α, β, and γ, and has GDP bound. The α-subunit (chain A) of the protein is a chimera of $G_{\alpha t}$ of bovine and $G_{\alpha i}$ of rat. A comparative model was constructed that consists entirely of the $G_{\alpha i}$ rat sequence using the sequence alignment shown in Fig. S5. The sequence alignment shows an extension of the N-terminal α-helix by one winding (four-residue gap) that was built in the comparative model as a straight α-helix. The Rosetta side chain construction algorithm (1) was then used to convert the appropriate residues of 1GOT into $G_{\alpha i}$ sequence, yielding a comparative model termed $G_{\alpha i}$-1GOT. The command line options used are shown below:

fixbb.linuxgccrelease -database -in:file:s -out:file:fullatom –resfile -out:prefix

Superposition of the Transducin C-Terminal Helix with the Opsin-Bound Peptide Ligand. The structure of G-protein coupled receptor opsin in complex with the C-terminal 11 residues of the α-subunit of the G-protein heterotrimer (PDB ID code 3DQB) was fused with the comparative model $G_{\alpha i}$-1GOT. Specifically, residues 344–347 in the α-subunit of the $G_{\alpha i}$-1GOT structure overlap in sequence with the first four residues of the peptide ligand in 3DQB (Fig. S6). Using these four overlapping residues, the heterotrimer was positioned relative to the receptor. This defines an initial position of the heterotrimer relative to the receptor. As already described by Scheerer et al. (2), this procedure positions portions of the heterotrimer in the membrane core in a nonphysical way.

In order to resolve the penetration of the heterotrimer into the membrane core, rotations of portions of the heterotrimer are performed at two pivot points. Subunits β and γ are rotated along with the N-terminal helix and switch-2 region of the α-subunit such that the resulting position of the N-terminal helix is approximately parallel with the membrane (40° rotation). A second rotation of 15° of the heterotrimer is applied at the junction of the 3DQB peptide and C-terminal helix of $G_{\alpha i}$-1GOT, moving the N-terminal helix parallel with the membrane.

The combination of these two rotations creates a physically realistic model that removes the β-, γ-subunits from the membrane core, places the N-terminal amphipathic helix parallel to the membrane surface, and puts the N terminus in a location that allows the alkyl chain of the myristoyl group and the nearby farnesylated C terminus of the γ-subunit to penetrate the membrane. The procedure results in chain breaks within the α-subunit and minor clashes in loop regions within the heterotrimer that are resolved via the Rosetta loop building protocol.

α-Helical Domain Docking. EPR distance measurements display a reorientation of the helical domain of the α-subunit when the heterotrimer binds to the receptor (Fig. 1). In order to capture this conformational motion, the α-helical domain was detached from the rest of the α-subunit by introduction of chain breaks between residues 59/60 and 184/185 of chain A of the $G_{\alpha i}$-1GOT structure. Next, a rigid body docking protocol was executed to sample possible placements of the helical domain with respect to the α-subunit. A total of 140,000 structures were created using Rosetta (3). The starting position of the α-helical domain was initially perturbed by up to 1.5 Å and 4° rotation. During docking trajectories translations of up to 0.05 Å and rotations of up to 2.5° were performed in a stepwise procedure. The command line flags used follow:

docking_protocol.linuxgccrelease -in:file:s start.pdb -out:nstruct 100 -docking:dock_pert 1.5 4 -docking:dock_mcm_trans_magnitude 0.05 -docking:dock_mcm_rot_magnitude 2.5 –out:overwrite

Filtering of α-Helical Domain Docking Models. Docking models were filtered for agreement with EPR distance data after docking. Agreement with the EPR distance restraints is calculated according to the knowledge-based potential given by Hirst et al. (4). Agreement can be expressed with a value between 0 (no agreement) and −1 (perfect agreement, Fig. S7*A*). In addition to the EPR distances, a filter was applied to ensure the chain break created at the cut points can be resolved through remodeling a minimal number of residues around the cut points. This filter minimizes the distances between residues 59/60 and 184/185 of the α-subunit of $G_{\alpha i}$-1GOT (Fig. S7*B*). The 1,000 models that pass both filters undergo a clustering analysis (Fig. S8), and the cluster center that agrees best with the experimental data is used for all further analysis (Table S1). This model shows a translation of approximately 8 Å and a rotation of 29° of the α-helical domain compared to its starting position.

The increased width in the distance distributions obtained from EPR spectroscopy (Fig. 1*C*) suggests a flexible relative orientation of the helical domain with respect to the heterotrimer in the receptor-bound state. The ensemble of 1,000 models in agreement with the EPR data might reflect part of this spatial disorder. A single model was selected to facilitate discussion of the general movement of the α-helical domain, as it is consistent between all models (Figs. S8 and S9). We conclude that this movement is well defined by the experimental data. Additional experimental measurements will be necessary to determine the parameters of the spatial disorder.

Rosetta loop building (5) and relaxation protocols (6) were utilized in order to reconnect the helical domain back to the rest of the α-subunit and refine the complex within the Rosetta energy functions. In addition, the αA helix (α-subunit residues 63–90) is unkinked in the model of the activated heterotrimer–receptor complex solely for demonstrative purposes of a possible mechanism of leverage for generating the helical domain movement (see main article).

1. Kuhlman B, et al. (2003) Design of a novel globular protein fold with atomic-level accuracy. *Science* 302:1364–1368.
2. Scheerer P, et al. (2008) Crystal structure of opsin in its G-protein-interacting conformation. *Nature* 455:497–502.
3. Gray JJ, et al. (2003) Protein-protein docking with simultaneous optimization of rigid-body displacements and side-chain conformations. *J Mol Biol* 331:281–299.
4. Hirst SJ, Alexander N, McHaourab HS, Meiler J (2011) An integrated tool for protein structure determination from sparse EPR data. *J Struct Biol* 173:506–514
5. Wang C, Bradley P, Baker D (2007) Protein-protein docking with backbone flexibility. *J Mol Biol* 373:503.
6. Misura KMS, Baker D. (2005) Progress and challenges in high-resolution refinement of protein structure models. *Proteins* 59:15–29.

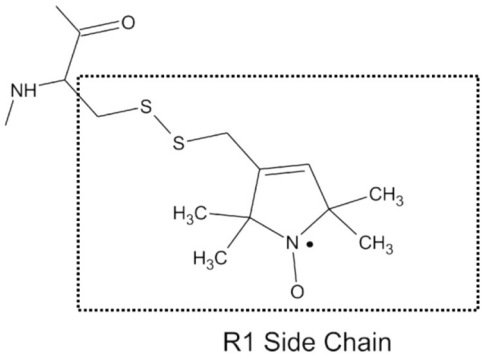

Fig. S1. The nitroxide R1 side chain.

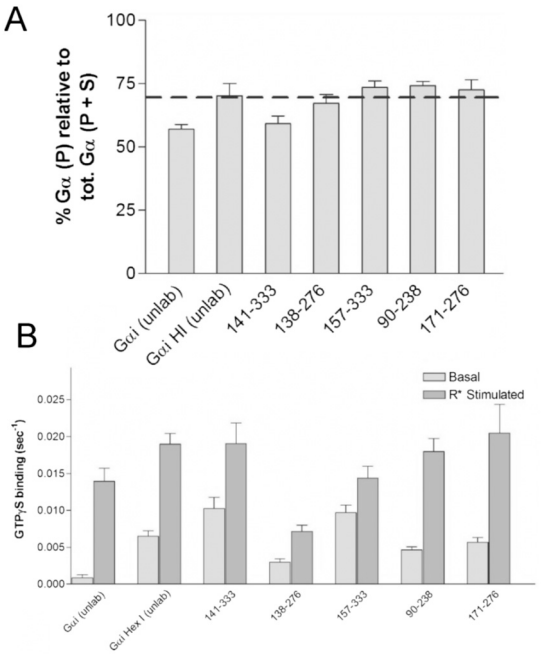

Fig. S2. (*A*) Binding of doubly spin-labeled mutants to rhodopsin in disc membranes. (*B*) Basal and receptor catalyzed nucleotide exchange rates for the doubly spin-labeled mutants. Assays were performed as described in *Methods*.

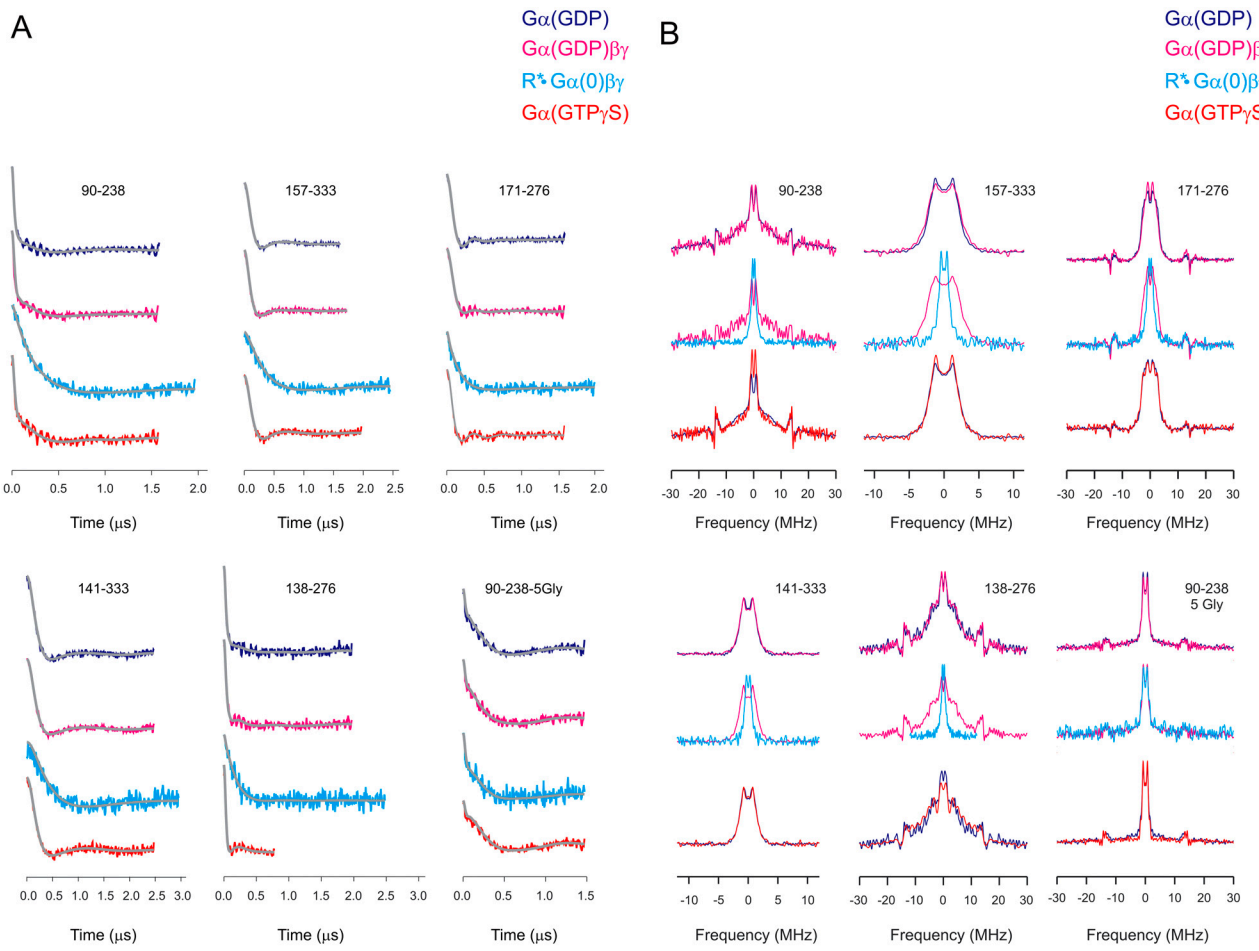

Fig. S3. (*A*) Background corrected dipolar evolution data for each double-labeled mutant along the activation pathway. Gray traces show fits to each individual dipolar evolution. (*B*) Fourier transformation of the dipolar evolution data given in *A* yields the dipolar spectra in *B*. The data are shown for each spin-labeled double mutant along the activation pathway.

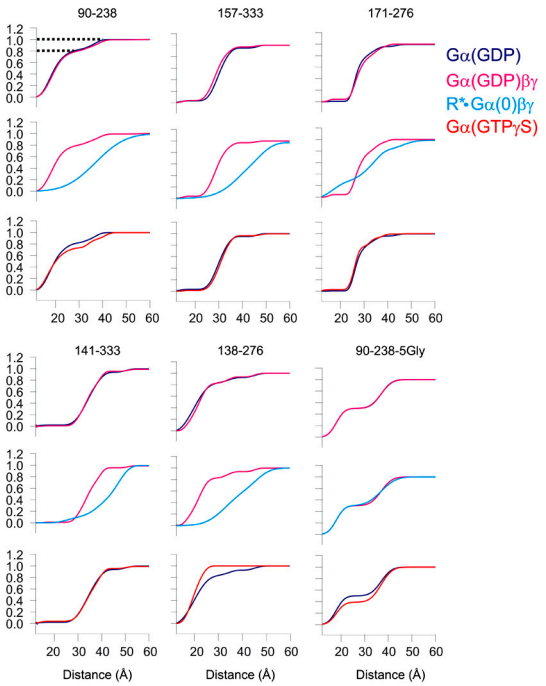

Fig. S4. Normalized integral representations of the distance distributions shown in Fig. 1*C* of the main text. Such representations are particularly useful for visually estimating the relative populations of the distances. This is illustrated, for example, in the top panel of the 90–238 mutant; the major population is about 80%. The most probable distance for a population is estimated from the midpoint of the transition.

```
Got/Goi chimera (1GOT)   1 MGAGASAEEK----HSRELEKKLKEDAEKDARTVKLLLLGAGESGKSTIVKQMKIIHQDG   56
Goi rat                  1 MGCTLSAEDKAAVERSKMIDRNLREDGEKAAREVKLLLLGAGESGKSTIVKQMKIIHEAG   60
Got/Goi chimera (1GOT)  57 YSLEECLEFIAIIYGNTLQSILAIVRAMTTLNIQYGDSARQDDARKLXHMADTIEEGTMP  116
Goi rat                 61 YSEEECKQYKAVVYSNTIQSIIAIIRAMGRLKIDFGDAARADDARQLFVLAGAAEEGFMT  120
Got/Goi chimera (1GOT) 117 KEMSDIIQRLWKDSGIQACFDRASEYQLNDSAGYYLSDLERLVTPGYVPTEQDVLRSRVK  176
Goi rat                121 AEIAGVIKRLWKDSGVQACFNRSREYQLNDSAAYYLNDLDRIAQPNYIPTQQDVLRTRVK  180
Got/Goi chimera (1GOT) 177 TTGIIETQFSFKDLNFRMFDVGGQRSERKKWIHCFEGVTAIIFCVALSDYDLVLAEDEEM  236
Goi rat                181 TTGIVETHFTFKDLHFKMFDVGGQRSERKKWIHCFEGVTAIIFCVALSDYDLVLAEDEEM  240
Got/Goi chimera (1GOT) 237 NRMHESMKLFDSICNNKWFTDTSIILFLNKKDLFEEKIKKSPLTICYPEYAGSNTYEEAG  296
Goi rat                241 NRMHESMKLFDSICNNKWFTDTSIILFLNKKDLFEEKIKKSPLTICYPEYAGSNTYEEAA  300
Got/Goi chimera (1GOT) 297 NYIKVQFLELNMRRDVKEIYSHMTCATDTQNVKFVFDAVTDIIIKENLKDCGLF        350
Goi rat                301 AYIQCQFEDLNKRKDTKEIYTHFTCATDTKNVQFVFDAVTDVIIKNNLKDCGLF        354
```

Fig. S5. A BLAST (Basic Local Alignment Search Tool) sequence alignment of $G\alpha_i$ and the $G\alpha_t/G\alpha_i$ chimera of 1GOT, which was used in comparative modeling. The sequence alignment features a single gap (red) within the N-terminal α-helix of the protein. The $G\alpha_i$ region (residues 216–294 of the 1GOT sequence) is shown in orange. The α-helical domain is shown in green. The C-terminal helix and 11 residues of the opsin-bound peptide are shown in yellow and blue, respectively.

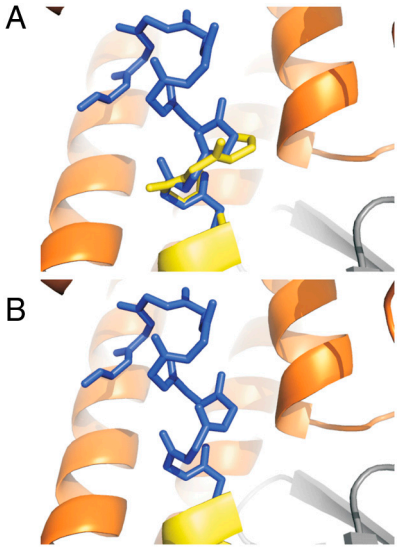

Fig. S6. Superposition of transducin's C-terminal helix with the opsin-bound peptide ligand. (*A*) The opsin structure is shown as orange ribbon with the 11 residue C-terminal peptide of transducin as blue sticks (PDB ID code 3DQB). The C terminus of the α-subunit of $G_{\alpha i}$-1GOT in yellow has been superimposed so that residues 344–347 overlap with the first four residues of the peptide. (*B*) The residues from the peptide are merged with $G_{\alpha i}$-1GOT by replacing residues 344–347 of the α-subunit with the first four residues of the peptide.

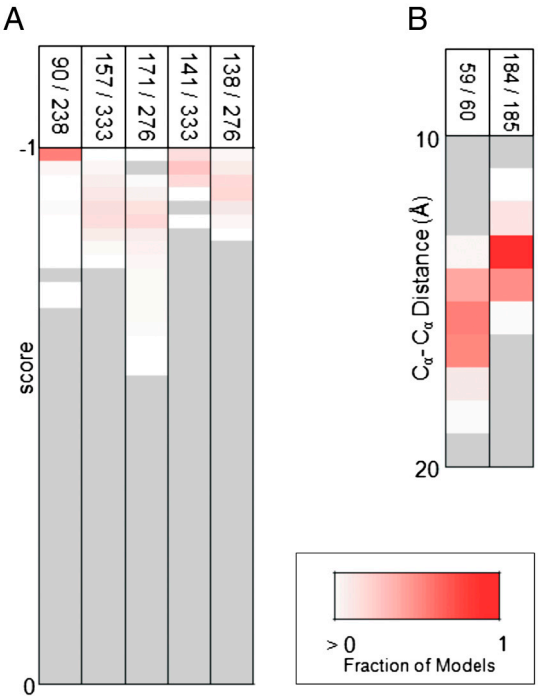

Fig. S7. The 1,000 models with repositioned helical domain filtered by EPR score and chain break distance. (*A*) The models were scored for agreement with the distance measurements according to the knowledge-based potential of Hirst et al. (4). The potential provides a score between −1 (perfect agreement) to zero (no agreement). Shown is the fraction of models for which a given score is observed for each EPR measurement. (*B*) It is important that the docking protocol does not introduce too large of a chain break between the helical domain and the rest of the α-subunit. Shown is the fraction of models with which a given C_α–C_α distance is observed for the two cut points. The distances were calculated before the chain breaks were removed, which was accomplished by reconstructing the linker regions between the helical domain and the rest of the α-subunit (5, 6). In both *A* and *B*, gray areas have counts of zero.

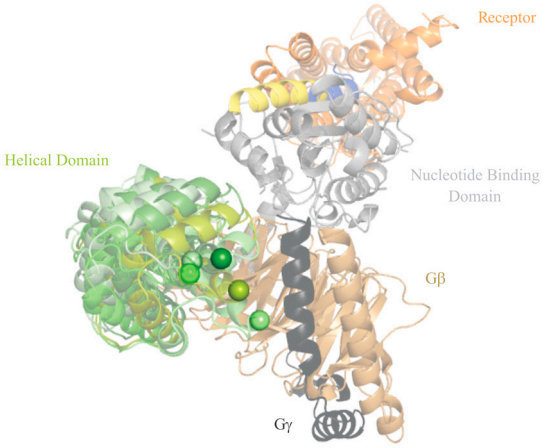

Fig. S8. The 1,000 models resulting from repositioning the helical domain were hierarchically clustered. A distance cutoff between clusters of 2.0 Å results in five cluster centers. Residue 90 is shown as alpha carbon spheres to guide the eye in distinguishing the different orientations of the helical domain. The cluster centers show relatively similar placements of the helical domain. The color coding shown above is similar to Fig. 3 in the main text. The C-terminal helix of the nucleotide binding domain is shown in yellow with its last 11 amino acids colored blue.

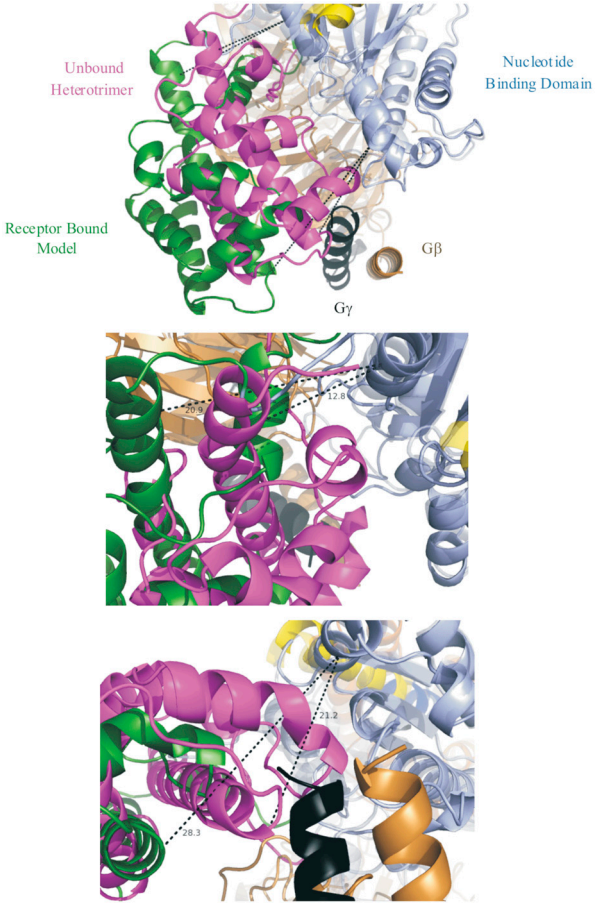

Fig. S9. Shown is the position of the helical domain in the unbound heterotrimer as determined from crystallography (PDB ID code 1GOT) (magenta ribbon) compared to the receptor-bound $G_{\alpha i}$-1GOT model (green ribbon). The relative positions of the two helical domains (model versus 1GOT structure) were determined by aligning the nucleotide binding domains of the α-subunit (light blue ribbon) in the two structures. (*Top*) The C_α–C_α distances at opposite ends of the helical domain were calculated in order to demonstrate the extent of the movement captured by the docking protocol. The distances were calculated between residues 51 and 66 (*Top*, dashed lines), and between residues 90 and 277 (*Bottom*, dashed lines). Coordinates of residues 51 and 277 outside the helical domain are used for reference. The helical domain is shown to rotate 29°. (*Middle*) The change in distance of residue 66 from residue 51 is 8.1 Å. (*Bottom*) The change in distance of residue 90 from residue 277 is 7.1 Å.

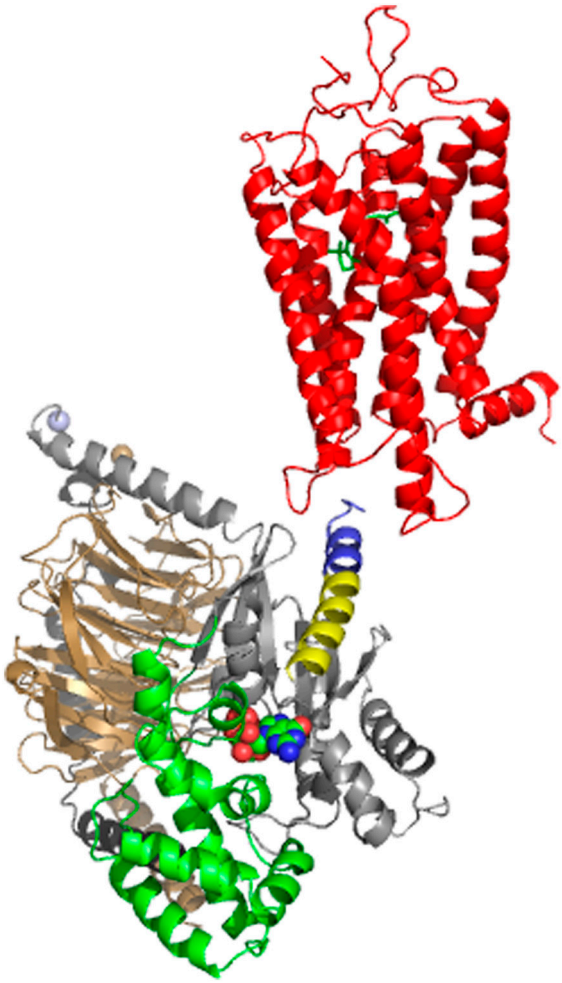

Movie S1. Animation showing the hypothesized conformational changes leading to GDP release. The crystal structure of rhodopsin before activation [red, PDB ID code 1U19 (1)] transitions to the activated state [orange, R*, PDB ID code 3DQB (2)]. The GDP-bound heterotrimer binds to R* and the helical domain of Gα(GDP) opens away from the nucleotide binding domain. The opening movement allows GDP release leading to $G_{\alpha}(0)_{\beta\gamma}$. Color scheme is G_{β}, tan; G_{γ}, black; G_{α}(GDP)helical domain, green; G_{α}(GDP)nucleotide binding domain, gray; GDP, spheres. The animation was created using Pymol RigiMOL (Schrodinger, LLC). Movie S1 (MOV)

1. Okada T, et al. (2004) The retinal conformation and its environment in rhodopsin in light of a new 2.2 Å crystal structure. *J Mol Biol* 342:571–583.
2. Scheerer P, et al. (2008) Crystal structure of opsin in its G-protein-interacting conformation. *Nature* 455:497–502.

Table S1. Agreement of the receptor-bound $G_{\alpha i}$-1GOT model with experimentally measured EPR distances

Mutant:	90/238	157/333	171/276	141/333	138/276
EPR experiment:					
Free heterotrimer	18 Å	28 Å	26 Å	33 Å	20 Å
Bound to activated receptor	38 Å	45 Å	34 Å	46 Å	34 Å
Distance change	20 Å	17 Å	8 Å	13 Å	14 Å
Structures:					
Free heterotrimer	11 Å	25 Å	23 Å	32 Å	16 Å
Bound to activated receptor	32 Å	40 Å	25 Å	41 Å	29 Å
Distance change	21 Å	15 Å	2 Å	9 Å	13 Å
Agreement between experiment and model according to KBP	−0.96	−0.96	−0.71	−0.96	−0.97

The EPR distances in the table are determined from the most probable distances in each distribution. The distances measured in models are measured between C_{β} atoms. Distances for the free heterotrimer were calculated using the experimental crystal structure (PDB ID code 1GOT). Distances for the receptor-bound state were calculated using the $G_{\alpha i}$-1GOT model. Distance agreement between the receptor-bound model and the EPR measurements were calculated according to the knowledge-based scoring potential (KBP) (4). Perfect agreement would be −1.0 and no agreement would be 0.0.